Negative Reactance Impacts on the Eigenvalues of the Jacobian Matrix in Power Flow and Type-1 Low-Voltage Power-Flow Solutions

Ding, Tao; Li, Cheng; Yang, Yongheng; Bo, Rui; Blaabjerg, Frede

Published in:
IEEE Transactions on Power Systems

DOI (link to publication from Publisher):
10.1109/TPWRS.2016.2645608

Publication date:
2017

Document Version
Accepted author manuscript, peer reviewed version

Negative Reactance Impacts on the Eigenvalues of the Jacobian Matrix in Power Flow and Type-1 Low-Voltage Power-Flow Solutions

Tao Ding, *Member, IEEE*, Cheng Li, *Student Member, IEEE*, Yongheng Yang, *Member, IEEE*
Rui Bo, *Senior Member, IEEE*, and Frede Blaabjerg, *Fellow, IEEE*

***Abstract*— It was usually considered in power systems that power flow equations had multiple solutions and all the eigenvalues of Jacobian matrix at the high-voltage operable solution should have negative real parts. Accordingly, type-1 low-voltage power flow solutions are defined in the case that the Jacobian matrix has only one positive real-part eigenvalue. However, an important issue which has not been well addressed yet is that the "negative reactance" may appear in the practical power system models. Thus, the negative real-part eigenvalues of the Jacobian matrix at the high-voltage operable solution may be positive and also the type-1 low-voltage solutions could have more than one positive real-part eigenvalues, being a major challenge. Therefore, in this paper, the recognition of the type-1 low-voltage power flow solutions is re-examined with the presence of negative reactance. Selected IEEE standard power system models and the real-world Polish power systems are then tested to verify the analysis. The results reveal that the negative reactance in the practical power systems has a significant impact on the negative real-part eigenvalues of the Jacobian matrix at the high-voltage operable solution as well as the number of positive real-part eigenvalues at the type-1 low-voltage power flow solutions.**

***Index Terms*— Negative reactance, power flow, continuation power flow, eigenvalues, type-1 power flow solution**

I. Introduction

It has been commonly considered that the power flow equations in power systems have multiple solutions [1]-[4]. The number of the power flow solutions depends on the system loading. The maximum number of solutions for an n-bus power system is estimated to be 2^{n-1}. Prior-art work has reported a vast array of methods to resolve the power flow equations and capture the multiple solutions [1]-[7].

Normally, tracking the multiple solutions of the power flow equations offers an effective way to analyze the static voltage stability [8]-[9], since the distance between the high-voltage operable power flow solution and the low-voltage solutions can be utilized as a static voltage stability index. When the system arrives at the maximum power transfer point, the operable high-voltage solution and low-voltage power flow solutions are coincident. When the distance is larger, the system is farther from the maximum power transfer point.

This work was supported by China Postdoctoral Science Foundation (2015M580847), the Independence research project of State Key Laboratory of Electrical Insulation and Power Equipment in Xi'an Jiaotong University (EIPE16301), Natural Science Basis Research Plan in Shaanxi Province of China (2016JQ5015).

T. Ding and C. Li are with the State Key Laboratory of Electrical Insulation and Power Equipment, School of Electrical Engineering, Xi'an Jiaotong University, Xi'an, 710049 Shaanxi, China (email: tding15@mail.xjtu.edu.cn).

Y. Yang and F. Blaabjerg are with the Department of Energy Technology, Aalborg University, DK-9220 Aalborg, Denmark (email: yoy@et.aau.dk; fbl@et.aau.dk).

Rui Bo is with the Midcontinent Independent Transmission System Operator (MISO), Eagan, MN 55121 USA (email: rui.bo@ieee.org).

Moreover, it is investigated that in [10]-[15] that the type-1 load-flow solutions are closely associated with the voltage instability phenomenon. Accordingly, the computational burden for the static voltage stability analysis can be significantly alleviated, when only considering the type-1 load-flow solutions. As a result, the static voltage stability indicator becomes the distance between the high-voltage operable power flow solution and the type-1 low-voltage power flow solutions.

Now, we will focus on how to find the type-1 low-voltage power flow solutions. According to the property of Type-1 power flow solutions, several methods have been proposed to acquire these solutions. In [16], a hybrid genetic and particle swarm optimization algorithm for locating all the type-1 power flow solutions has been adopted. Moreover, a state-space search method has been applied to calculate the low-voltage power flow solutions in ill-conditioned systems [17]. Additionally, a potential algorithm based on Continuation Power FLOW (CPFLOW) has been presented in [18] and [19].

However, recent study has revealed that negative reactance may appear in real-world power system models. For example, the IEEE 300-bus test system has one "negative reactance" in the MATPOWER [20]; three real-world Polish power systems, including 3012-bus, 3120-bus and 3375-bus systems, have more than 10 "negative reactances"; nearly 100 "negative reactances" exist in the U.S. Midwest ISO (MISO) EMS power system. Notably, the "negative reactance" mainly appears in actual systems induced by the process of system equivalencing or three winding transformer modeling [21]. From a purely physical perspective, transformer windings are taken as inductive rather than capacitive. However, due to the mutual effects between windings of the three-winding transformers and the virtual system equivalencing, small negative values may appear in the mid-voltage side windings. In some cases, the series compensators used to increase the transfer capability in transmission lines may also result in negative reactance. Additionally, negative reactance is introduced deliberately to simulate the power breaker operation [22].

The presence of the negative reactance even with limited number and small value may result in that a) the eigenvalues of Jacobian matrix at the high-voltage operable solution may have positive real parts and b) the type-1 low-voltage power flow solutions may have more than one real-part eigenvalues. This poses a challenge to the traditional definition of type-1 low-voltage power flow solutions and the viewpoint that the Jacobian matrix at the high-voltage solution has all of its eigenvalues with negative real parts in [18].

It should be noted that this phenomenon is very critical to track the low-voltage solutions of the power flow equations,

especially for the type-1 power flow solutions. However, such an issue has never been addressed in the state-of-the-art. In light of the above issues, the impact of negative reactance on the eigenvalues of the converged Jacobian matrix at the high-voltage operable solution as well as the type-1 low-voltage power flow solutions has been explored in this paper.

To the authors' best knowledge, the main contributions of the paper can be summarized as follows:

- It has rigorously proved that the power flow Jacobian matrix has all of its eigenvalues with negative real parts at high-voltage operable solution without considering negative reactance.
- The impact of negative reactance on the eigenvalues of the power flow Jacobian matrix at high-voltage operable solution has been evaluated.
- The definition of type-1 low-voltage power flow solutions in [18] has been re-examined.

The rest of the paper is organized as follows: The eigenvalues of the power flow Jacobian matrix are explored in Section II, followed by the investigation of the negative reactance effects on the recognition of the type-1 low-voltage power flow solutions. In Section III, some discussions on the new findings are presented. Section IV provides case studies on selected IEEE standard systems and practical Polish power systems considering negative reactance. Finally, Section V draws the conclusions.

II. Eigenvalues of the Power Flow Jacobian Matrix

A. Definition of the Power Flow Jacobian Matrix

Typically, the power flow equations can be formulated as

$$\begin{cases} P_i = U_i \sum_{j=1}^{n} U_j \left(G_{ij} \cos\theta_{ij} + B_{ij} \sin\theta_{ij} \right) \\ Q_i = U_i \sum_{j=1}^{n} U_j \left(G_{ij} \sin\theta_{ij} - B_{ij} \cos\theta_{ij} \right) \end{cases} \tag{1}$$

where n is the number of buses; P_i and Q_i are the injected active and reactive power at bus i; U_i and θ_i are the voltage magnitude and angle at bus i; $\theta_{ij}=\theta_i-\theta_j$; G_{ij} and B_{ij} are real and imaginary parts of the admittance matrix at the i-th row and the j-th column, with

$$G_{ij} + \mathrm{j}B_{ij} = -\left(g_{ij} + \mathrm{j}b_{ij} \right) = \frac{-r_{ij}}{r_{ij}^2 + x_{ij}^2} + \mathrm{j}\frac{x_{ij}}{r_{ij}^2 + x_{ij}^2} \tag{2}$$

$$G_{ii} + \mathrm{j}B_{ii} = -\sum_{j=1, j\neq i}^{n} \left(G_{ij} + \mathrm{j}B_{ij} \right) + \left(g_{sh,i} + \mathrm{j}b_{sh,i} \right) \tag{3}$$

in which $g_{sh,i}$ and $b_{sh,i}$ denote the shunt-connected elements at bus i. Commonly, the power flow can be solved by Newton-Raphson method, where the voltage magnitude and angle corrections can be obtained by the Jacobian matrix. It should be noted that it is usually convenient for numerical solution to normalize the voltage magnitude correction, so the normalized Newton equations can be formulated as

$$\begin{bmatrix} \Delta \boldsymbol{P} \\ \Delta \boldsymbol{Q} \end{bmatrix} = -\begin{bmatrix} \dfrac{\partial \boldsymbol{P}}{\partial \boldsymbol{\theta}} & \boldsymbol{U}\dfrac{\partial \boldsymbol{P}}{\partial \boldsymbol{U}} \\ \dfrac{\partial \boldsymbol{Q}}{\partial \boldsymbol{\theta}} & \boldsymbol{U}\dfrac{\partial \boldsymbol{Q}}{\partial \boldsymbol{U}} \end{bmatrix} \begin{bmatrix} \Delta \boldsymbol{\theta} \\ \Delta \boldsymbol{U}/\boldsymbol{U} \end{bmatrix} \tag{4}$$

where $\Delta\boldsymbol{P}$ and $\Delta\boldsymbol{Q}$ are the mismatched active and reactive power; $\Delta\boldsymbol{U}$ and $\Delta\boldsymbol{\theta}$ are the error of the voltage magnitudes and angles. Here, the Jacobian matrix of the normalized Newton equations is given by

$$\boldsymbol{J} = -\begin{bmatrix} \dfrac{\partial \boldsymbol{P}}{\partial \boldsymbol{\theta}} & \boldsymbol{U}\dfrac{\partial \boldsymbol{P}}{\partial \boldsymbol{U}} \\ \dfrac{\partial \boldsymbol{Q}}{\partial \boldsymbol{\theta}} & \boldsymbol{U}\dfrac{\partial \boldsymbol{Q}}{\partial \boldsymbol{U}} \end{bmatrix} = \begin{bmatrix} -\dfrac{\partial \boldsymbol{P}}{\partial \boldsymbol{\theta}} & -\boldsymbol{U}\dfrac{\partial \boldsymbol{P}}{\partial \boldsymbol{U}} \\ -\dfrac{\partial \boldsymbol{Q}}{\partial \boldsymbol{\theta}} & -\boldsymbol{U}\dfrac{\partial \boldsymbol{Q}}{\partial \boldsymbol{U}} \end{bmatrix} = \begin{bmatrix} \boldsymbol{H} & \boldsymbol{N} \\ \boldsymbol{M} & \boldsymbol{L} \end{bmatrix} \tag{5}$$

where

$$H_{ij} = -\frac{\partial P_i}{\partial \theta_j} = \begin{cases} U_i U_j \left(B_{ij}\cos\theta_{ij} - G_{ij}\sin\theta_{ij} \right) & i \neq j \\ Q_i + U_i^2 B_{ii} & i = j \end{cases} \tag{6}$$

$$N_{ij} = -U_j \frac{\partial P_i}{\partial U_j} = \begin{cases} -U_i U_j \left(G_{ij}\cos\theta_{ij} + B_{ij}\sin\theta_{ij} \right) & i \neq j \\ -P_i - U_i^2 G_{ii} & i = j \end{cases} \tag{7}$$

$$M_{ij} = -\frac{\partial Q_i}{\partial \theta_j} = \begin{cases} U_i U_j \left(G_{ij}\cos\theta_{ij} + B_{ij}\sin\theta_{ij} \right) & i \neq j \\ -P_i + U_i^2 G_{ii} & i = j \end{cases} \tag{8}$$

$$L_{ij} = -U_j \frac{\partial Q_i}{\partial U_j} = \begin{cases} U_i U_j \left(B_{ij}\cos\theta_{ij} - G_{ij}\sin\theta_{ij} \right) & i \neq j \\ -Q_i + U_i^2 B_{ii} & i = j \end{cases} \tag{9}$$

B. Assumptions

In order to study the eigenvalues of power flow Jacobian matrix, the following mild assumptions for a transmission network under the normal steady state operation have been made [23]-[24]:

(i) Voltage magnitudes (U) at the buses are close to 1.0 p.u., i.e., $U \approx 1.0$ p.u. > 0;

(ii) The voltage angle differences among the bus voltages are quite small, i.e., $|\theta_{ij}| \approx 0$, $\sin\theta_{ij} \approx \theta_{ij} \approx 0$, and $\cos\theta_{ij} \approx 1$;

(iii) The injected reactive power at any bus is always much less than the reactive power consumed by the components connected to this bus when they are short-circuited to the ground, such that $|Q_i| << |B_{ii}U_i^2|$.

(iv) The shunt admittances of the transmission line b_s are very small and the eigenvalues of the sub-matrices $\boldsymbol{H}$ and $\boldsymbol{L}$ are hardly affected by the small values Q_i/U_i^2 and $b_{s,i}$, such that it satisfies $\left\| \dfrac{\lambda(\overline{\boldsymbol{H}}^{\dagger}) - \lambda(\overline{\boldsymbol{H}}^{\diamond})}{\lambda(\overline{\boldsymbol{H}}^{\diamond})} \right\| < 1$ and $\left\| \dfrac{\lambda(\overline{\boldsymbol{L}}^{\dagger}) - \lambda(\overline{\boldsymbol{L}}^{\diamond})}{\lambda(\overline{\boldsymbol{L}}^{\diamond})} \right\| < 1$, where $\lambda(\overline{\boldsymbol{H}}^{\diamond})$ and $\lambda(\overline{\boldsymbol{L}}^{\diamond})$ are eigenvalues of sub-matrix $\boldsymbol{H}$ and $\boldsymbol{L}$ without small values; $\lambda(\overline{\boldsymbol{H}}^{\dagger})$ and $\lambda(\overline{\boldsymbol{L}}^{\dagger})$ are eigenvalues of sub-matrix $\boldsymbol{H}$ and $\boldsymbol{L}$ with small values.

C. Preliminaries

When it comes to the eigenvalues of the matrix, it is usually associated with the matrix definiteness. However, the definiteness of the matrix is generally defined for the Hermitian matrix. The reason is that the Hermitian matrix uniquely corresponds to a quadratic real function and has sound properties, such as its eigenvalues are all real numbers, and the negative definiteness is equivalent to the fact that all the eigenvalues are negative. In order to investigate the eigenvalues of the asymmetric matrices, the definiteness of the Hermitian part of the asymmetric matrices by the following Corollary 1 will be employed in the analysis.

Definition 1[25]: An $n\times n$ Hermitian matrix $\boldsymbol{A}$ is negative definite, if and only if $\boldsymbol{x}^H\boldsymbol{A}\boldsymbol{x}<0$ for any nonzero complex vector $\boldsymbol{x}\in\mathcal{C}^{n\times 1}$, where $\boldsymbol{x}^H$ is the conjugate transpose of $\boldsymbol{x}$.

Corollary 1: An asymmetric real matrix $\boldsymbol{A}$ will have negative real-part eigenvalues, if the Hermitian part $\left(\boldsymbol{A}+\boldsymbol{A}^T\right)/2$ is negative definite.

The proof of corollary can be found in Appendix A, and it should be noted that the condition "$\left(\boldsymbol{A}+\boldsymbol{A}^T\right)/2$ is negative definite" is a sufficient but not necessary one for the case that "An asymmetric real matrix $\boldsymbol{A}$ is negative definite".

In addition, three theorems for the further study on the eigenvalues have been provided in following:

(**Gershgorin Circle Theorem**) [26] Let $\boldsymbol{A}$ be an $n\times n$ matrix, with entries a_{ij}. For every eigenvalue of $\boldsymbol{A}$ denoted by λ, lies within at least one of the Gershgorin discs, such that $\left|\lambda-a_{ii}\right|\le\sum_{j\ne i}\left|a_{ij}\right|$.

(**Schur Complements Theorem**)[26] For any symmetric matrix, $\boldsymbol{M}$, with $\boldsymbol{M}=\begin{bmatrix}\boldsymbol{A} & \boldsymbol{B}\\ \boldsymbol{B}^T & \boldsymbol{C}\end{bmatrix}$, if $\boldsymbol{A}$ is invertible, it holds that $\boldsymbol{M}\prec\boldsymbol{0}$, if and only if $\boldsymbol{A}\prec\boldsymbol{0}$ and $\boldsymbol{C}-\boldsymbol{B}^T\boldsymbol{A}^{-1}\boldsymbol{B}\prec\boldsymbol{0}$.

D. Negative Real-Part Eigenvalues of the Jacobian Matrix with Positive Reactance at the High-Voltage Solution

It is commonly considered that the reactance is always positive for all the lines, i.e., $x_{ij}>0$. As a result, $G_{ij}<0$ and $B_{ij}>0$ for $i\ne j$; $G_{ii}>0$ and $B_{ii}<0$ for $i=j$. Hereafter, it will be shown that *the real parts of all eigenvalues of the Jacobian matrix at the high-voltage operable solution are negative.*

Proof: It can be easily observed in (5) that the Jacobian matrix is an asymmetric real matrix. Now, we will define its Hermitian part $\left(\boldsymbol{J}+\boldsymbol{J}^T\right)/2$ as

$$\left(\boldsymbol{J}+\boldsymbol{J}^T\right)/2=\begin{bmatrix}\left(\boldsymbol{H}+\boldsymbol{H}^T\right)/2 & \left(\boldsymbol{N}+\boldsymbol{M}^T\right)/2\\ \left(\boldsymbol{N}^T+\boldsymbol{M}\right)/2 & \left(\boldsymbol{L}+\boldsymbol{L}^T\right)/2\end{bmatrix}=\begin{bmatrix}\boldsymbol{H}^\dagger & \boldsymbol{K}\\ \boldsymbol{K}^T & \boldsymbol{L}^\dagger\end{bmatrix} \quad (10)$$

where

$$H_{ij}^\dagger=\frac{H_{ij}+H_{ij}^T}{2}=\begin{cases}U_iU_jB_{ij}\cos\theta_{ij} & i\ne j\\ Q_i+U_i^2B_{ii} & i=j\end{cases} \quad (11)$$

$$K_{ij}=\frac{N_{ij}+M_{ij}^T}{2}=\begin{cases}-U_iU_jB_{ij}\sin\theta_{ij} & i\ne j\\ -P_i & i=j\end{cases} \quad (12)$$

$$L_{ij}^\dagger=\frac{L_{ij}+L_{ij}^T}{2}=\begin{cases}U_iU_jB_{ij}\cos\theta_{ij} & i\ne j\\ -Q_i+U_i^2B_{ii} & i=j\end{cases} \quad (13)$$

In the matrix form, (12) can be reformulated as

$$\left(\boldsymbol{J}+\boldsymbol{J}^T\right)/2=\begin{bmatrix}\boldsymbol{H}^\dagger & \boldsymbol{K}\\ \boldsymbol{K}^T & \boldsymbol{L}^\dagger\end{bmatrix}=\begin{bmatrix}\boldsymbol{U}_P & \boldsymbol{0}\\ \boldsymbol{0} & \boldsymbol{U}_Q\end{bmatrix}\overline{\boldsymbol{J}}\begin{bmatrix}\boldsymbol{U}_P & \boldsymbol{0}\\ \boldsymbol{0} & \boldsymbol{U}_Q\end{bmatrix} \quad (14)$$

where $\boldsymbol{U}_P=diag\left(U_1,...,U_{mp}\right)$, $\boldsymbol{U}_Q=diag\left(U_1,...,U_{mq}\right)$ with the subscripts mp and mq indicating the number of buses related to the active power and reactive power equations, respectively. Meanwhile, the elements of matrix $\overline{\boldsymbol{J}}=\begin{bmatrix}\overline{\boldsymbol{H}}^\dagger & \overline{\boldsymbol{K}}\\ \overline{\boldsymbol{K}}^T & \overline{\boldsymbol{L}}^\dagger\end{bmatrix}$ follow as

$$\overline{H}_{ij}^\dagger=\begin{cases}B_{ij}\cos\theta_{ij} & i\ne j\\ Q_i/U_i^2+B_{ii} & i=j\end{cases},\ \overline{K}_{ij}=\begin{cases}-B_{ij}\sin\theta_{ij} & i\ne j\\ -P_i/U_i^2 & i=j\end{cases},\ \overline{L}_{ij}^\dagger=\begin{cases}B_{ij}\cos\theta_{ij} & i\ne j\\ -Q_i/U_i^2+B_{ii} & i=j\end{cases} \quad (15)$$

Now, we will focus on the definiteness of the matrix $\left(\boldsymbol{J}+\boldsymbol{J}^T\right)/2$ considering that the reactance of all the lines is positive and three steps are presented as follows:

(1) To show the sub-matrices $\overline{\boldsymbol{H}}^\dagger$ and $\overline{\boldsymbol{L}}^\dagger$ are negative definite

At first, we construct two new matrices $\overline{\boldsymbol{H}}^\diamond$ and $\overline{\boldsymbol{L}}^\diamond$, with ignoring the small value $\left|Q_i/U_i^2\right|$ and the shunt admittances b_s in *Assumption* (iii) and (iv), which gives

$$\overline{H}_{ij}^\diamond=\begin{cases}B_{ij}\cos\theta_{ij} & i\ne j\\ -\sum_{j=1,j\ne i}^{n}B_{ij} & i=j\end{cases},\qquad \overline{L}_{ij}^\diamond=\begin{cases}B_{ij}\cos\theta_{ij} & i\ne j\\ -\sum_{j=1,j\ne i}^{n}B_{ij} & i=j\end{cases} \quad (16)$$

where the two matrices satisfy

$$\left|\overline{H}_{ii}^\diamond\right|=\sum_{j=1,j\ne i}^{n}\left|B_{ij}\right|>\sum_{j=1,j\ne i}^{n}\left|B_{ij}\cos\theta_{ij}\right|\ge\sum_{j=1,j\ne i}^{n}B_{ij}\cos\theta_{ij}=\sum_{j=1,j\ne i}^{n}\overline{H}_{ij}^\diamond \quad (17)$$

$$\left|\overline{L}_{ii}^\diamond\right|=\sum_{j=1,j\ne i}^{n}\left|B_{ij}\right|>\sum_{j=1,j\ne i}^{n}\left|B_{ij}\cos\theta_{ij}\right|\ge\sum_{j=1,j\ne i}^{n}B_{ij}\cos\theta_{ij}=\sum_{j=1,j\ne i}^{n}\overline{L}_{ij}^\diamond \quad (18)$$

Then, it can be found from (17) and (18) that both the matrices $\overline{\boldsymbol{H}}^\diamond$ and $\overline{\boldsymbol{L}}^\diamond$ are strictly diagonally dominant. Applying the ***Gershgorin Circle Theorem*** concludes that both $\overline{\boldsymbol{H}}^\diamond$ and $\overline{\boldsymbol{L}}^\diamond$ are negative definite.

Furthermore, according to *Assumption* (iv), it leads to

$$\left|\lambda\left(\overline{\boldsymbol{H}}^\dagger\right)-\lambda\left(\overline{\boldsymbol{H}}^\diamond\right)\right|<\left|\lambda\left(\overline{\boldsymbol{H}}^\diamond\right)\right| \quad (19)$$

Since $\overline{\boldsymbol{H}}^\diamond$ is negative definite, all the eigenvalues of $\overline{\boldsymbol{H}}^\diamond$ are negative, which means $\lambda\left(\overline{\boldsymbol{H}}^\diamond\right)<0$, thus (21) implies

$$\lambda\left(\overline{\boldsymbol{H}}^\dagger\right)<\lambda\left(\overline{\boldsymbol{H}}^\diamond\right)+\left|\lambda\left(\overline{\boldsymbol{H}}^\diamond\right)\right|=\lambda\left(\overline{\boldsymbol{H}}^\diamond\right)-\lambda\left(\overline{\boldsymbol{H}}^\diamond\right)=0 \quad (20)$$

It can be observed that all the eigenvalues of $\overline{\boldsymbol{H}}^\dagger$ are negative, so the sub-matrix $\overline{\boldsymbol{H}}^\dagger$ is negative definite. Moreover, the same conclusion can be obtained for the sub-matrix $\overline{\boldsymbol{L}}^\dagger$.

(2) To show the matrix $\overline{\boldsymbol{J}}$ is negative definite

For any given vector $\begin{pmatrix}\boldsymbol{a}\\ \boldsymbol{b}\end{pmatrix}\ne\boldsymbol{0}$, we will arrive at

$$\begin{pmatrix}\boldsymbol{a}^T & \boldsymbol{b}^T\end{pmatrix}\begin{bmatrix}\overline{\boldsymbol{H}}^\dagger & \overline{\boldsymbol{K}}\\ \overline{\boldsymbol{K}}^T & \overline{\boldsymbol{L}}^\dagger\end{bmatrix}\begin{pmatrix}\boldsymbol{a}\\ \boldsymbol{b}\end{pmatrix}=\boldsymbol{a}^T\overline{\boldsymbol{H}}^\dagger\boldsymbol{a}+\boldsymbol{b}^T\overline{\boldsymbol{L}}^\dagger\boldsymbol{b}+2\boldsymbol{a}^T\overline{\boldsymbol{K}}\boldsymbol{b} \quad (21)$$

Since $\overline{\boldsymbol{H}}^\dagger$ and $\overline{\boldsymbol{L}}^\dagger$ are negative definite, it holds for $\lambda_{\max}\left(\overline{\boldsymbol{H}}^\dagger\right)<0$ and $\lambda_{\max}\left(\overline{\boldsymbol{L}}^\dagger\right)<0$. Meanwhile, we can obtain that $\boldsymbol{a}^T\overline{\boldsymbol{H}}^\dagger\boldsymbol{a}\le\lambda_{\max}\left(\overline{\boldsymbol{H}}^\dagger\right)\boldsymbol{a}^T\boldsymbol{a}<0$ and $\boldsymbol{b}^T\overline{\boldsymbol{L}}^\dagger\boldsymbol{b}\le\lambda_{\max}\left(\overline{\boldsymbol{L}}^\dagger\right)\boldsymbol{b}^T\boldsymbol{b}<0$.

Then, (21) becomes

$$\begin{pmatrix}\boldsymbol{a}^T & \boldsymbol{b}^T\end{pmatrix}\begin{bmatrix}\overline{\boldsymbol{H}}^\dagger & \overline{\boldsymbol{K}}\\ \overline{\boldsymbol{K}}^T & \overline{\boldsymbol{L}}^\dagger\end{bmatrix}\begin{pmatrix}\boldsymbol{a}\\ \boldsymbol{b}\end{pmatrix}\le\lambda_{\max}\left(\overline{\boldsymbol{H}}^\dagger\right)\boldsymbol{a}^T\boldsymbol{a}+\lambda_{\max}\left(\overline{\boldsymbol{L}}^\dagger\right)\boldsymbol{b}^T\boldsymbol{b}+2\boldsymbol{a}^T\overline{\boldsymbol{K}}\boldsymbol{b} \quad (22)$$

According to *Assumptions* (i) and (ii), the active power flow equation of (1) can be approximated to be $P_i\approx U_i\sum_{j=1}^{n}U_jB_{ij}\sin\theta_{ij}$. In addition, $\sin\theta_{ij}\approx\theta_{ij}\approx 0$ and $\left|\theta_{ij}\right|\le\varepsilon$, where ε is a small num-

ber, so $\left|\overline{\boldsymbol{K}}_{ij}\right| \le \mathcal{O}(\varepsilon)$ can be achieved. Here, where the operator $\mathcal{O}(\cdot)$ denotes the order of magnitude and we will have

$$2\left|\boldsymbol{a}^T \overline{\boldsymbol{K}} \boldsymbol{b}\right| \le 2\mathcal{O}(\varepsilon)\left|\boldsymbol{a}^T \boldsymbol{b}\right| \le 2\mathcal{O}(\varepsilon)\|\boldsymbol{a}\|\|\boldsymbol{b}\| \tag{23}$$

Furthermore, (22) will become

$$\begin{aligned}
&\begin{pmatrix}\boldsymbol{a}^T & \boldsymbol{b}^T\end{pmatrix}\begin{bmatrix}\overline{\boldsymbol{H}}^{\dagger} & \overline{\boldsymbol{K}} \\ \overline{\boldsymbol{K}}^T & \overline{\boldsymbol{L}}^{\dagger}\end{bmatrix}\begin{pmatrix}\boldsymbol{a} \\ \boldsymbol{b}\end{pmatrix} \\
&\le \lambda_{\max}\left(\overline{\boldsymbol{H}}^{\dagger}\right)\boldsymbol{a}^T\boldsymbol{a} + \lambda_{\max}\left(\overline{\boldsymbol{L}}^{\dagger}\right)\boldsymbol{b}^T\boldsymbol{b} + 2\boldsymbol{a}^T\overline{\boldsymbol{K}}\boldsymbol{b} \\
&\le \lambda_{\max}\left(\overline{\boldsymbol{H}}^{\dagger}\right)\boldsymbol{a}^T\boldsymbol{a} + \lambda_{\max}\left(\overline{\boldsymbol{L}}^{\dagger}\right)\boldsymbol{b}^T\boldsymbol{b} + 2\mathcal{O}(\varepsilon)\|\boldsymbol{a}\|\|\boldsymbol{b}\| \qquad (24) \\
&\le \left(\lambda_{\max}\left(\overline{\boldsymbol{H}}^{\dagger}\right) + \mathcal{O}(\varepsilon)\right)\boldsymbol{a}^T\boldsymbol{a} + \left(\lambda_{\max}\left(\overline{\boldsymbol{L}}^{\dagger}\right) + \mathcal{O}(\varepsilon)\right)\boldsymbol{b}^T\boldsymbol{b} \\
&\le 0
\end{aligned}$$

As shown above, for any nonzero vector, (24) will hold, so $\overline{\boldsymbol{J}}$ is a negative definite matrix.

(3) To show the matrix $\left(\boldsymbol{J}+\boldsymbol{J}^T\right)/2$ is negative definite

Since $\overline{\boldsymbol{J}}$ is negative definite, $\overline{\boldsymbol{J}}$ can be decomposed by the Cholesky decomposition into $\overline{\boldsymbol{J}} = -\overline{\boldsymbol{W}}^T\overline{\boldsymbol{W}}$, leading to

$$\left(\boldsymbol{J}+\boldsymbol{J}^T\right)/2 = \begin{bmatrix}\boldsymbol{H}^{\dagger} & \boldsymbol{K} \\ \boldsymbol{K}^T & \boldsymbol{L}^{\dagger}\end{bmatrix} = -\left(\overline{\boldsymbol{W}}\begin{bmatrix}\boldsymbol{U}_P & \boldsymbol{0} \\ \boldsymbol{0} & \boldsymbol{U}_Q\end{bmatrix}\right)^T\left(\overline{\boldsymbol{W}}\begin{bmatrix}\boldsymbol{U}_P & \boldsymbol{0} \\ \boldsymbol{0} & \boldsymbol{U}_Q\end{bmatrix}\right) \prec \boldsymbol{0} \tag{25}$$

Therefore, the matrix $\left(\boldsymbol{J}+\boldsymbol{J}^T\right)/2$ is negative definite.

Furthermore, according to Corollary 1, we can obtain that the real parts of all eigenvalues of the Jacobian matrix $\boldsymbol{J}$ at the high-voltage operable solution are negative, since the Hermitian part $\left(\boldsymbol{J}+\boldsymbol{J}^T\right)/2$ is negative definite.

(Q.E.D.)

E. Eigenvalues of the Jacobian Matrix Considering the Negative Reactance at the High-Voltage Solution

However, as discussed in Section I, there may be "negative reactance" in the power systems, i.e., x_{ij}<0, which will break the diagonally dominant property of both matrices $\overline{\boldsymbol{H}}^{\dagger}$ and $\overline{\boldsymbol{L}}^{\dagger}$, and therefore the negative definiteness of $\overline{\boldsymbol{J}}$ will be affected. Let's take the matrix $\overline{\boldsymbol{H}}^{\dagger}$ for an example in the following.

If the reactance of one branch is negative (e.g., x_{ij}<0), the diagonal value increases but the off-diagonal value decreases, i.e., $\overline{\boldsymbol{H}}^{\dagger}_{ii} \uparrow$ and $\overline{\boldsymbol{H}}^{\dagger}_{ij} \downarrow$. With the increase of the absolute value of the negative reactance, the diagonal dominance will not be attained anymore. It is clear that the reactance as $x_{ij} = x'_{ij} - \mu$ can be formulated, where x'_{ij} and μ are strictly positive. Thus, the imaginary part of the admittance matrix formed by $\boldsymbol{x}$ and $\boldsymbol{x}$' can be written as $\boldsymbol{B}$ and $\boldsymbol{B}'$, respectively.

$$B_{ij} = \frac{x_{ij}}{r_{ij}^2 + x_{ij}^2} < 0,\ B'_{ij} = \frac{x'_{ij}}{r_{ij}^2 + \left(x'_{ij}\right)^2} > 0,\ B_{ij} = B'_{ij} - \alpha,\ \alpha > 0 \tag{26}$$

$$B_{ii} < 0, \quad B_{ii} = B'_{ii} + \alpha \tag{27}$$

At first, let $\overline{\boldsymbol{H}}^{\dagger}_{+}$ be formed with only positive reactance. With respect to the results in the last subsection, the matrix $\overline{\boldsymbol{H}}^{\dagger}_{+}$ is strictly negative definite, such that $\overline{\boldsymbol{H}}^{\dagger}_{+} \prec 0$. Furthermore, the original matrix $\overline{\boldsymbol{H}}^{\dagger}$ is formed with both negative and positive reactance. Here, we take one negative reactance for illustration and it is possible to reorder the bus index in such a way that the bus i and j are the last two rows/columns. Then, the original matrix $\overline{\boldsymbol{H}}^{\dagger}$ can be derived by

$$\overline{\boldsymbol{H}}^{\dagger} = \overline{\boldsymbol{H}}^{\dagger}_{+} + \begin{bmatrix}\boldsymbol{0} & \boldsymbol{0} \\ \boldsymbol{0} & \begin{bmatrix}\alpha & -\alpha\cos\theta_{ij} \\ -\alpha\cos\theta_{ij} & \alpha\end{bmatrix}\end{bmatrix} = \begin{bmatrix}\boldsymbol{H}_{+} & \boldsymbol{C} \\ \boldsymbol{C}^T & \begin{bmatrix}h_{ii}+\alpha & h_{ij}-\alpha\cos\theta_{ij} \\ h_{ij}-\alpha\cos\theta_{ij} & h_{jj}+\alpha\end{bmatrix}\end{bmatrix} \tag{28}$$

where $\boldsymbol{H}_{+}$ and $\boldsymbol{C}$ are sub-matrix of $\overline{\boldsymbol{H}}^{\dagger}_{+}$; α is a parameter that can be adjusted to match the value of the negative reactance. Since x_{ij} is negative, according to (26) and the *Assumption* (ii), α can be approximated to

$$\alpha = B'_{ij} - B_{ij} \approx 1/x'_{ij} - 1/x_{ij} = 1/x'_{ij} + 1/\left|x_{ij}\right| \tag{29}$$

which shows that α is increasing with the decrease of $|x_{ij}|$.

Furthermore, the negative definiteness of $\overline{\boldsymbol{H}}^{\dagger}_{+}$ implies that $\boldsymbol{H}_{+}$ is negative definite as well, according to **Schur Complements Theorem**. Thus, the definiteness of $\overline{\boldsymbol{H}}^{\dagger}$ is determined by the definiteness of the matrix $\begin{bmatrix}h_{ii}+\alpha & h_{ij}-\alpha\cos\theta_{ij} \\ h_{ij}-\alpha\cos\theta_{ij} & h_{jj}+\alpha\end{bmatrix} - \boldsymbol{C}^T\boldsymbol{H}_{+}^{-1}\boldsymbol{C}$. If this matrix is negative definite, $\overline{\boldsymbol{H}}^{\dagger}$ will be negative definite, otherwise, the definiteness of $\overline{\boldsymbol{H}}^{\dagger}$ cannot be determined. Moreover, the definiteness of the matrix $\begin{bmatrix}h_{ii}+\alpha & h_{ij}-\alpha\cos\theta_{ij} \\ h_{ij}-\alpha\cos\theta_{ij} & h_{jj}+\alpha\end{bmatrix} - \boldsymbol{C}^T\boldsymbol{H}_{+}^{-1}\boldsymbol{C}$ is shown in Appendix B, which implies that larger α (i.e., smaller value of "negative reactance", x_{ij}) leads to a higher possibility for the loss of negative definiteness of $\overline{\boldsymbol{H}}^{\dagger}$. As the example of "negative reactance" shows in Section I, negative reactance mostly results from the 3-winding transformer modeling and its value is generally small. Therefore, it is highly possible that the negative definiteness of $\overline{\boldsymbol{H}}^{\dagger}$ will be lost when there is "negative reactance" in the practical power system model. In addition, the loss of the definiteness of $\overline{\boldsymbol{H}}^{\dagger}$ will result in the indefiniteness of the Hermitian part $\left(\boldsymbol{J}+\boldsymbol{J}^T\right)/2 = \begin{bmatrix}\boldsymbol{H}^{\dagger} & \boldsymbol{K} \\ \boldsymbol{K}^T & \boldsymbol{L}^{\dagger}\end{bmatrix}$.

Since Corollary 1 is a sufficient but not necessary condition, it is not possible to confirm whether the real part of all the eigenvalues of the Jacobian matrix $\boldsymbol{J}$ at the high-voltage operable solution is negative. However, the counterpart from the single-load stiff-bus test system in Appendix C implies that some negative real-part eigenvalues of the Jacobian matrix at a high-voltage operable solution may become positive.

Therefore, considering the negative reactance, the distribution of the eigenvalues of the Jacobian matrix at the high-voltage operable solution is determined by the value of negative reactance: when $\left|x_{ij}\right|$ is large, $\left(\boldsymbol{J}+\boldsymbol{J}^T\right)/2 = \begin{bmatrix}\boldsymbol{H}^{\dagger} & \boldsymbol{K} \\ \boldsymbol{K}^T & \boldsymbol{L}^{\dagger}\end{bmatrix}$ can still keep negative definite and the real part of all the eigenvalues of the Jacobian matrix $\boldsymbol{J}$ at the high-voltage operable solution is still negative. Nevertheless, with decreasing $\left|x_{ij}\right|$, the

negative definiteness of $\left(\boldsymbol{J}+\boldsymbol{J}^{T}\right)/2=\begin{bmatrix}\boldsymbol{H}^{\dagger} & \boldsymbol{K}\\ \boldsymbol{K}^{T} & \boldsymbol{L}^{\dagger}\end{bmatrix}$ will be lost, which may lead to the loss of negative real-part eigenvalues.

III. Discussions on the New Findings

It has been observed that the existence of negative reactance lines may shift the real part of some eigenvalues of the Jacobian matrix away from negative values to positive ones. This leads to a phenomenon that the power flow solution is a high-voltage operable solution, but the Jacobian matrix may have positive real-part eigenvalues.

From the simple example of the single-load stiff-bus test system in Appendix C, it can be found in the closed form of eigenvalues of (C4) that, on the condition that power flow has a high-voltage solution, $E-2U\cos\theta\le 0$, the eigenvalues $\lambda(J)\ge 0$ if the reactance is negative (i.e., x<0). At the same time, one eigenvalue in the converged Jacobian matrix has a negative real part at low-voltage solution. Therefore, the Jacobian matrix at type-1 low voltage power flow solutions in this example has less than one positive real-part eigenvalue.

Furthermore, the CPFLOW method in [18] and [27] has been employed to track the high-voltage operable and low-voltage type-1 power flow solutions on large-scale test systems. Specifically, the CPFLOW technique utilizes a predictor-corrector scheme to trace a solution path by the parameterized power flow equations. With an increase of load levels, it is indicated that the system state moves towards the maximum power transfer point, where the Jacobian matrix becomes singular. The simulations in the next section show that the power flow solution is still a high-voltage operable solution but the Jacobian matrix has positive real-part eigenvalues, when considering the negative reactance. Moreover, the type-1 low-voltage power flow solutions could have more than one positive real-part eigenvalues in the converged Jacobian matrix. It means that one positive eigenvalue of the converged Jacobian matrix does not necessarily produce the type-1 low-voltage power flow solutions.

The result therefore challenges the analysis of Jacobian matrix of high-voltage operable solution and the definition of type-1 low-voltage power flow solution in [18] that:

1) If the power flow solution is a high-voltage operable solution, the Jacobian matrix has all of its eigenvalues with negative real-part;

2) A type-1 low-voltage power flow solution has a single positive real-part eigenvalue, and the others are negative real-part eigenvalues.

From the proofs in Section II, we can conclude the following statement with the consideration of the negative reactance that:

1) When there is no negative reactance, all the eigenvalues of the Jacobian matrix at the high-voltage power flow solution have negative real parts; when there exists negative reactance, the power flow solution may still be a high-voltage operable one even when there are positive real-part eigenvalues in the converged Jacobian matrix. The number of positive real-part eigenvalues is related to the value of the negative reactance;

2) The definition of the type-1 low- voltage solution should be revised as: the power flow solution is a type-1 low-voltage solution, if the number of the positive real-part eigenvalues in the converged Jacobian matrix is one different from that at the high-voltage operable solution.

IV. Numerical Results

A. Negative Reactance/Eigenvalues of the Jacobian Matrix

In order to track the phenomenon of the negative reactance and positive real-part eigenvalues, eight IEEE standard test systems and eight real-world Polish power systems from MATPOWER [20] are studied. The results are presented in Table I, where NNR is the number of negative reactance and NPE is the number of positive real-part eigenvalues. It can be observed in Table I that the IEEE 300-bus system has one negative reactance of $x_{120\text{-}1201}$=-0.3697 p.u.. For the three real-world Polish power systems, 3012-bus and 3120-bus both have 10 negative reactances, and 3375-bus has 12 negative reactances. Besides, the Jacobian matrix with the consideration of negative reactances is not negative definite anymore and the number of positive real-part eigenvalues is just twice the number of negative reactances. Meanwhile, the power flow solutions are all high-voltage solutions, the voltage magnitudes of which are all around a reasonable level (a.k.a., $U\approx$1.0 p.u.). Furthermore, the assumption (iv) in Section I is also tested on the aforementioned systems, which can be shown in Table I, where two indexes are introduced as

$$\eta(\boldsymbol{H})=\max_i\left\|\frac{\lambda_i\left(\overline{\boldsymbol{H}}^{\dagger}\right)-\lambda_i\left(\overline{\boldsymbol{H}}^{\diamond}\right)}{\lambda_i\left(\overline{\boldsymbol{H}}^{\diamond}\right)}\right\| \text{ and } \eta(\boldsymbol{L})=\max_i\left\|\frac{\lambda_i\left(\overline{\boldsymbol{L}}^{\dagger}\right)-\lambda_i\left(\overline{\boldsymbol{L}}^{\diamond}\right)}{\lambda_i\left(\overline{\boldsymbol{L}}^{\diamond}\right)}\right\| \quad (31)$$

Observe that both $\eta(\boldsymbol{H})$ and $\eta(\boldsymbol{L})$ are smaller than one, and in particular, $\eta(\boldsymbol{H})$ is generally much smaller, which implies that the given assumption (iv) can be satisfied in all the IEEE standard systems and eight real-world Polish power systems.

TABLE I. NNRs and Positive Real-Part Eigenvalues at the SEP.

Systems	NNR	NPEs	*Assumption* (iv)	
			$\eta(\boldsymbol{H})$	$\eta(\boldsymbol{L})$
case9	0	0	0.037387	0.074711
case14	0	0	0.001022	0.001598
case24	0	0	0.016896	0.114992
case30	0	0	0.001520	0.011292
case39	0	0	0.035173	0.128342
case57	0	0	0.004327	0.042389
case118	0	0	0.001296	0.172236
case300	1	2	0.027426	0.209606
case2383wp	0	0	0.010719	0.431781
case2736sp	0	0	0.006802	0.579896
case2737sop	0	0	0.004921	0.441467
case2746wop	0	0	0.006279	0.544575
case2746wp	0	0	0.009216	0.515809
case3012wp	10	20	0.008046	0.689393
case3120sp	10	20	0.008701	0.433149
case3375wp	12	24	0.007910	0.640185

B. Discussions on the Type-1 Solutions

In this section, three systems are taken as examples to demonstrate the number of positive real-part eigenvalues at the Type-1 low-voltage solutions using the CPFLOW-based algorithm a 5-bus system [18]. It can be found in [18] that the reactance of each line in the 5-bus system is positive, and the Jacobian matrix at the high-voltage power solution has all of its eigenvalues with negative real parts and the type-1 low-voltage solutions have only one positive real-part eigenvalue. In order

to study the effect of the negative reactance on the eigenvalues of power flow Jacobian matrix, the results of a 5-bus test system are presented as follows:

Example 1: Considering negative reactance with a small value, assume that there is one negative reactance of 0.01-0.03*j* p.u. on the line #3-#5. The high-voltage and four type-1 low-voltage power flow solutions are presented in Table II. Furthermore, the eigenvalues of the converged Jacobian matrix at each power flow solution are shown in Table III. It can be observed that there are two positive real-part eigenvalues in the Jacobian matrix at the high-voltage power solution. Moreover, each type-1 lower-voltage power flow solution has three positive real-part eigenvalues, which is one more than that at the high-voltage solution.

TABLE II. HIGH-VOLTAGE AND TYPE-1 LOW-VOLTAGE POWER FLOW SOLUTIONS OF THE FIRST 5-BUS SYSTEM WITH.

	high-voltage solution	Type-1 low-voltage power flow solutions			
		1	2	3	4
θ_1	0.0000	0.0000	0.0000	0.0000	0.0000
θ_2	-1.9913	-25.1520	-12.0965	-25.8125	-138.4805
θ_3	-4.3739	-70.3519	-10.9785	-142.8122	-133.3012
θ_4	-5.4821	-31.7546	-70.7742	-39.9153	-141.4626
θ_5	-4.8360	-131.9410	-15.4707	-62.7795	-130.8539
U_1	1.0600	1.0600	1.0600	1.0600	1.0600
U_2	1.0000	1.0000	1.0000	1.0000	1.0000
U_3	0.9783	0.0226	0.7848	0.2619	0.4759
U_4	0.9666	0.6300	0.0570	0.5861	0.7925
U_5	0.9797	0.3587	0.7490	0.0276	0.5994

TABLE III. IMPACT OF NEGATIVE REACTANCE ON THE EIGENVALUES OF THE JACOBIAN MATRIX OF THE FIRST 5-BUS SYSTEM.

High-voltage solution	Type-1 solution 1	Type-1 solution 2
49.7122 - 22.0919j	-18.5509	34.7429 - 14.6580j
49.7122 + 22.0919j	-7.0812	34.7429 + 14.6580j
-35.9010	6.4495 - 1.0085j	-23.7665
-12.3484 - 4.0607j	6.4495 + 1.0085j	3.1571
-12.3484 + 4.0607j	2.5314	-6.2326
-3.9087	-3.4561	-4.6117
-6.9766	-1.7360	-1.8780
Type-1 solution 3	**Type-1 solution 4**	
-17.8059	21.2837 - 6.3550j	
6.6389 - 0.8429j	21.2837 + 6.3550j	
6.6389 + 0.8429j	7.9611	
-6.2457	-9.4403 - 3.0521j	
-3.3880	-9.4403 + 3.0521j	
1.4794	-3.9546 - 1.5537j	
-1.2101	-3.9546 + 1.5537j	

Example 2: For the same 5-bus system with a large value of negative reactance, it is assumed that the value of the negative reactance on the line #3-#5 is 0.01-2.50j p.u.. Then, the high-voltage power flow solution and four type-1 low-voltage power flow solutions obtained as presented in Table IV. Furthermore, the eigenvalues of the converged Jacobian matrix at each power flow solution are shown in Table V. At this time, all the eigenvalues of the Jacobian matrix at high-voltage power solution are negative and each type-1 lower-voltage power flow solution has one positive real-part eigenvalues.

Example 1 and example 2 have demonstrated that if negative reactance is taken into account, the Jacobian matrix evaluated at high voltage solution may have positive real-part eigenvalue and the Jacobian matrix at type-1 low-voltage power flow solutions may have more than one positive real-part eigenvalue.

TABLE IV. HIGH-VOLTAGE AND TYPE-1 LOW-VOLTAGE POWER FLOW SOLUTIONS OF THE SECOND 5-BUS SYSTEM.

	high-voltage solution	Type-1 low-voltage power flow solutions			
		1	2	3	4
θ_1	0.0000	0.0000	0.0000	0.0000	0.0000
θ_2	-2.3826	-10.1736	-12.4792	-8.5795	-137.5970
θ_3	-6.6012	-72.7246	-22.5132	-13.3323	-142.6252
θ_4	-6.4961	-17.6694	-72.8108	-12.8270	-141.9442
θ_5	-3.5480	-8.5719	-9.3610	-54.3564	-109.6997
U_1	1.0600	1.0600	1.0600	1.0600	1.0600
U_2	1.0000	1.0000	1.0000	1.0000	1.0000
U_3	0.9593	0.0566	0.5218	1.0097	1.0001
U_4	0.9597	0.6339	0.0636	0.9768	0.9734
U_5	0.9960	1.0327	1.0106	0.0540	0.1961

TABLE V. IMPACT OF NEGATIVE REACTANCES ON THE EIGENVALUES OF THE JACOBIAN MATRIX OF THE SECOND 5-BUS SYSTEM.

High-voltage solution	Type-1 solution 1	Type-1 solution 2
-35.8017	-26.8977	-24.0107
-12.8987 - 4.1888j	-8.2182 - 2.5290j	-7.8734 - 2.1038j
-12.8987 + 4.1888j	-8.2182 + 2.5290j	-7.8734 + 2.1038j
-3.2410	-7.0685	2.8867
-5.7881	1.9320	-4.0221
-7.8767 - 2.4698j	-3.9044	-1.6027
-7.8767 + 2.4698j	-1.3777	-2.7712
Type-1 solution 3	**Type-1 solution 4**	
-30.5733	7.7729	
-13.4389 - 4.3542j	-13.7930 - 4.4974j	
-13.4389 + 4.3542j	-13.7930 + 4.4974j	
3.3922	-8.0664 - 1.6039j	
-5.8476	-8.0664 + 1.6039j	
-3.2464	-0.5397	
-1.2053	-2.0280	

Example 3: In order to show the impact of the values of negative reactance on the number of the Jacobian matrix's positive real-part eigenvalues, another test system is adopted from the IEEE 14-bus system, where it is assumed that there are two negative reactances on the line #4-#7 and #4-#9. Five cases are considered with the different values of negative reactances:

- In case 1, the values of negative reactance are very small, i.e., ($x_{4\text{-}7}$=-0.01, $x_{4\text{-}9}$=-0.01) p.u.;
- In case 2, the values of negative reactance are small, i.e., ($x_{4\text{-}7}$=-0.06, $x_{4\text{-}9}$=-0.04) p.u.;
- In case 3, the values of negative reactance are large, i.e., ($x_{4\text{-}7}$=-0.20, $x_{4\text{-}9}$=-0.20) p.u.;
- In case 4, the values of negative reactance are further properly increased, i.e., ($x_{4\text{-}7}$=-0.40, $x_{4\text{-}9}$=-1.20) p.u.;
- In case 5, the values of negative reactance are very large, i.e., ($x_{4\text{-}7}$=-2.00, $x_{4\text{-}9}$=-2.00) p.u..

Furthermore, it has been investigated in Fig.1 that the voltage magnitudes are all around an operable high voltage level (a.k.a., U≈1.0 p.u.). Meanwhile, the eigenvalues of the converged Jacobian matrix at the high-voltage solution are shown in Table VI. It can be observed that the converged Jacobian matrix at the high-voltage power solution may not be negative definite and the number of positive real-part eigenvalues is related to the value negative reactances. With the increase of the absolute value of negative reactances, the number of positive real-part eigenvalues decrease. In addition, Table VII shows the number of positive real-part eigenvalues of converged Jacobian matrix at the type-1 lower-voltage power flow solution under different cases. It should be noted that there are 2(n-1) type-1 low-voltage power flow solutions where n is the number of buses. Here, it should be pointed out that only one

solution is chosen for illustration due to the limited space. Compared with Table VI, the results shows that the number of positive real-part eigenvalues at the type-1 low-voltage solution is just one more than that at the high-voltage power flow solution.

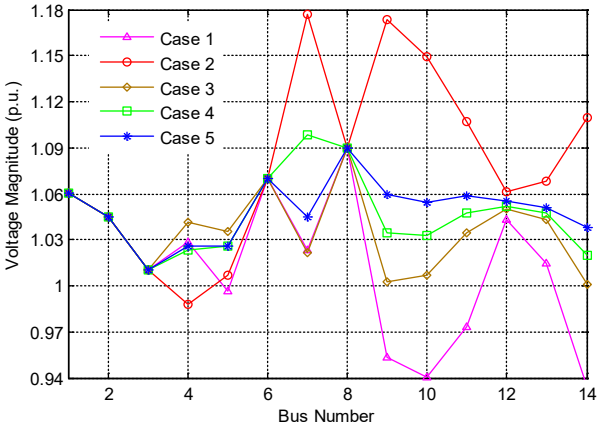

Fig. 1. Voltage magnitude of high-voltalge solution under five cases.

TABLE VI. EIGENVALUES AT THE HIGH-VOLTAGE SOLUTION.

Case 1	Case 2	Case 3
303.10 ± 5.02j	48.7464 ± 4.7782j	-54.5945 ± 17.2144j
8.95 ± 0.91j	-48.7873 ± 15.1293j	-35.3052
-45.45 ± 13.05j	-34.4661	-29.4030 ± 8.6498j
-34.04	-24.2866 ± 9.1192j	-21.8658
-21.98 ± 7.78j	-20.7440	4.3007 ± 0.6516j
-20.43	-12.9425 ± 7.7446j	-12.8575 ± 7.7444j
-13.03 ± 7.73j	-12.7523	-15.2495 ± 1.3277j
-11.32 ± 2.75j	-10.7157 ± 3.3903j	-11.9028 ± 3.2260j
-0.74	0.6478	-0.8538
-7.77	-0.7789	-3.2547
-6.35 ± 2.37j	-1.8941	-5.9931 ± 2.1947j
-5.75 - 1.94j	-7.4268 ± 1.6286j	-5.2272 ± 1.7749j
-4.69	-4.9772 ± 0.9950j	-7.6271
-3.90	-5.8024 ± 1.9843j	-5.9866
Case 4	Case 5	
-53.9798 ± 16.5669j	-55.9779 ± 17.1343j	
-40.0281 ± 9.5363j	-35.2998	
-34.9330	-30.1682 ± 6.9648j	
-22.1717	-21.4763	
-19.9434 ± 1.6430j	-16.8828 ± 2.3285j	
-13.5484 ± 7.9717j	-12.3246 ± 7.5514j	
-12.6662 ± 3.2243j	-12.8227 ± 2.8377j	
0.5632	-8.5350 ± 2.4381j	
-1.3154 ± 0.3678j	-0.0843	
-9.3942 ± 1.9163j	-1.2895	
-6.6272 ± 2.7418j	-2.1357	
-4.1814	-4.6235 ± 1.8305j	
-5.6765 ± 1.5351j	-6.0791 ± 1.1053j	
	-4.1448	

TABLE VII. EIGENVALUES AT ONE TYPE-1 LOW-VOLTAGE POWER FLOW SOLUTIONS.

Case 1	Case 2	Case 3
257.75	47.1891 ± 4.8702j	-46.4757 ± 14.5778j
235.38	-44.2053 ± 13.8557j	-27.2208
66.41	-32.0892	-18.5953
62.71	-26.4901 ± 10.0755j	-11.0329 ± 6.8632j
-38.72 ± 10.89j	-11.9494 ± 3.6340j	-12.8089
-31.70	-11.9208	2.0102 ± 0.7040j
-19.19 ± 6.88j	-9.8607 ± 3.8747j	-9.1812 ± 0.9426j
-17.06	-9.2031	0.2882
-8.68 ± 5.81j	-6.3488	-0.5164
-10.05 ± 2.36j	-4.4908 ± 2.1015j	-1.6473
1.86	-4.8069	-2.6620 ± 1.0635j
-0.40	-2.0361	-4.1240 ± 1.4259j
-0.69	1.7036	-6.4449 ± 1.9056j
-2.61	0.8978	-6.7000 ± 0.3817j
-5.51 ± 1.57j	-0.5772	
-6.81	-0.2155	
-5.76		
Case 4	Case 5	
-57.7633 ± 17.9048j		
-35.4528	-37.3825 ± 9.8909j	
-18.6534	-33.7383 ± 7.9777j	
-15.9574	-24.9589	
-8.7394 ± 5.8119j	-19.9537	
-12.2248 ± 2.6068j	-18.5792 ± 2.2882j	
-12.7834	-12.7928 ± 7.6786j	
-9.7943 ± 1.5026j	-9.6053 ± 2.5729j	
-6.3993	0.3233	
-5.3256 ± 1.7983j	-0.0927	
-4.0958	-1.6703	
-2.6879	-1.9826	
1.3271	-8.2229	
0.5098	-6.3295 ± 2.0035j	
-1.1116	-5.0568 ± 1.9136j	
-0.4356	-4.9731	
-0.5924		

V. CONCLUSIONS

This paper has presented an important phenomenon in the practical power system models, in which "negative reactance" may appear. As a consequence, the negative real-part eigenvalues of the Jacobian matrix at the high-voltage operable solution may be lost and the type-1 low-voltage power flow solutions may have more than one positive real-part eigenvalues, which imposes major challenges to the conventional viewpoints. The results from several study cases have demonstrated that:

a) The power flow solution with positive real-part eigenvalues in the converged Jacobian matrix may still be an operable solution due to the existence of negative reactance. The number of the positive real-part eigenvalues is related to the values of the negative reactance.

b) The power flow solution will be a type-1 low-voltage one, if the number of the positive real-part eigenvalues in the converged Jacobian matrix is one different from that at the high-voltage solution.

ACKNOWLEDGEMENT

The authors would like to thank the six reviewers and the editor for the valuable suggestions and comments which have improved the quality of this work. In addition, the authors would also like to thank Professor Dr. Jiaqing Yang from the Department of Mathematics, Xi'an Jiaotong University for giving us some constructive suggestions.

APPENDIX

A. To Show the Corollary 1

Proof: For any eigenvalue of a given asymmetric real matrix $\boldsymbol{A}$, denoted by λ, it gives

$$\boldsymbol{A}\boldsymbol{y} = \lambda \boldsymbol{y} \tag{A1}$$

Furthermore, pre-multiplying $\boldsymbol{y}^H$ for both sides of (A1) yields

$$\begin{cases} \boldsymbol{y}^H \boldsymbol{A}\boldsymbol{y} = \boldsymbol{y}^H \lambda \boldsymbol{y} \\ \left(\boldsymbol{y}^H \boldsymbol{A}\boldsymbol{y}\right)^H = \left(\boldsymbol{y}^H \lambda \boldsymbol{y}\right)^H \Rightarrow \boldsymbol{y}^H \boldsymbol{A}^H \boldsymbol{y} = \boldsymbol{y}^H \lambda^H \boldsymbol{y} \end{cases} \tag{A2}$$

Since $\boldsymbol{A}$ is a real matrix, $\boldsymbol{A}^H=\boldsymbol{A}^T$, and it holds for

$$\boldsymbol{y}^H\boldsymbol{A}^T\boldsymbol{y}=\boldsymbol{y}^H\lambda^H\boldsymbol{y} \tag{A3}$$

$$\boldsymbol{y}^H\boldsymbol{y}\frac{\left(\lambda^H+\lambda\right)}{2}=\boldsymbol{y}^H\frac{\left(\boldsymbol{A}+\boldsymbol{A}^T\right)}{2}\boldsymbol{y} \tag{A4}$$

According to Definition 1, $\boldsymbol{y}^H\frac{\left(\boldsymbol{A}+\boldsymbol{A}^T\right)}{2}\boldsymbol{y}<0$ is valid. Moreover, $\boldsymbol{y}^H\boldsymbol{y}>0$ and $\mathrm{Re}(\lambda)=\left(\lambda^H+\lambda\right)/2$, so $\mathrm{Re}(\lambda)<0$.

(Q.E.D.)

B. To Show the Definiteness of $\begin{bmatrix} h_{ii}+\alpha & h_{ij}-\alpha\cos\theta_{ij} \\ h_{ij}-\alpha\cos\theta_{ij} & h_{jj}+\alpha \end{bmatrix}-\boldsymbol{C}^T\boldsymbol{H}_+^{-1}\boldsymbol{C}$

Let the determinant function be

$$f_\alpha(\lambda)=\det\left(\begin{bmatrix}\lambda & 0\\ 0 & \lambda\end{bmatrix}-\begin{bmatrix} h_{ii}+\alpha & h_{ij}-\alpha\cos\theta_{ij} \\ h_{ij}-\alpha\cos\theta_{ij} & h_{jj}+\alpha \end{bmatrix}+\boldsymbol{C}^T\boldsymbol{H}_+^{-1}\boldsymbol{C}\right)=0 \tag{B1}$$

Since $\overline{\boldsymbol{H}}_+^{\dagger}$ is negative definite, (B2) can be derived when considering the ***Schur Complements Theorem***.

$$\begin{bmatrix} h_{ii} & h_{ij} \\ h_{ij} & h_{jj} \end{bmatrix}-\boldsymbol{C}^T\boldsymbol{H}_+^{-1}\boldsymbol{C}=\begin{bmatrix} a & b \\ b & c \end{bmatrix}\prec\boldsymbol{0} \tag{B2}$$

which leads to $a<0$, $c<0$ and $ac-b^2>0$.

Furthermore, (B1) can be reformulated as

$$f_\alpha(\lambda)=\det\left(\begin{bmatrix}\lambda & 0\\ 0 & \lambda\end{bmatrix}-\begin{bmatrix} a+\alpha & b-\alpha\cos\theta_{ij} \\ b-\alpha\cos\theta_{ij} & c+\alpha \end{bmatrix}\right)=0 \tag{B3}$$

Thus, the eigenvalues can then be calculated by

$$\lambda(\alpha)=\begin{cases}\lambda_+(\alpha)=\dfrac{a+c}{2}+\alpha+\sqrt{\left(\dfrac{a-c}{2}\right)^2+\left(\alpha\cos\theta-b\right)^2} \\ \lambda_-(\alpha)=\dfrac{a+c}{2}+\alpha-\sqrt{\left(\dfrac{a-c}{2}\right)^2+\left(\alpha\cos\theta-b\right)^2}\end{cases} \tag{B4}$$

Subsequently, the condition shown in (B5) should hold, which also shows that λ is monotonously increasing along with the adjustable parameter α.

$$\partial\lambda/\partial\alpha=1\pm\left|\left(\alpha\cos\theta-b\right)\right|\cos\theta\Big/\sqrt{\left(\frac{a-c}{2}\right)^2+\left(\alpha\cos\theta-b\right)^2}\ge 0 \tag{B5}$$

Moreover, we can obtain that

When $\alpha\to+\infty$, it yields

$$\lambda_\pm(+\infty)=\alpha\pm\alpha\cos\theta=+\infty>0 \tag{B6}$$

When $\alpha\to-\infty$, it yields

$$\lambda_\pm(-\infty)=\alpha\pm\alpha\cos\theta=-\infty<0 \tag{B7}$$

As a result, the sign of the eigenvalues $\lambda_\pm(\alpha)$ are related to the value of α, which gives the fact that the definiteness of the matrix $\begin{bmatrix} h_{ii}+\alpha & h_{ij}-\alpha\cos\theta_{ij} \\ h_{ij}-\alpha\cos\theta_{ij} & h_{jj}+\alpha \end{bmatrix}-\boldsymbol{C}^T\boldsymbol{H}_+^{-1}\boldsymbol{C}$ is related to the value of α as well. Moreover, a larger α leads to a higher possibility for the loss of negative definiteness of $\begin{bmatrix} h_{ii}+\alpha & h_{ij}-\alpha\cos\theta_{ij} \\ h_{ij}-\alpha\cos\theta_{ij} & h_{jj}+\alpha \end{bmatrix}-\boldsymbol{C}^T\boldsymbol{H}_+^{-1}\boldsymbol{C}$.

C. Eigenvalues of the Single-Load Stiff-Bus Test System

A widely used single-load stiff-bus test system is shown in Fig. 2, where the power flow equation can be written as

$$\begin{cases}EU\left(g\cos\theta+b\sin\theta\right)-U^2g=P_L \\ U^2b-EU\left(b\cos\theta-g\sin\theta\right)=Q_L\end{cases} \tag{C1}$$

where E is the grid voltage amplitude, P_L and Q_L are the load active power and reactive power, respectively, θ is the bus voltage angle, with

$$g+\mathrm{j}b=\frac{1}{r+\mathrm{j}x}\Rightarrow g=\frac{r}{r^2+x^2},b=\frac{-x}{r^2+x^2} \tag{C2}$$

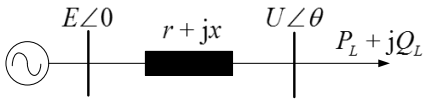

Fig. 2. A single-load stiff-bus test system.

The Jacobian matrix of (C1) is then formulated as

$$J=-\begin{bmatrix}\dfrac{\partial P}{\partial\theta} & U\dfrac{\partial P}{\partial U} \\ \dfrac{\partial Q}{\partial\theta} & U\dfrac{\partial Q}{\partial U}\end{bmatrix}=\begin{bmatrix}EU\left(b\cos\theta-g\sin\theta\right) & -2gU^2+EU\left(g\cos\theta+b\sin\theta\right) \\ EU\left(g\cos\theta+b\sin\theta\right) & EU\left(g\sin\theta-b\cos\theta\right)+2bU^2\end{bmatrix} \tag{C3}$$

Following, the closed form of eigenvalues can be obtained as

$$\begin{aligned}\lambda(J)&=bU^2\pm U\sqrt{b^2U^2+E\left(b^2+g^2\right)\left(E-2U\cos\theta\right)} \\ &=\frac{U^2}{r^2+x^2}\left(-x\pm\sqrt{x^2+\frac{E\left(r^2+x^2\right)}{U^2}\left(E-2U\cos\theta\right)}\right)\end{aligned} \tag{C4}$$

Notably, if the power flow equation has a high-voltage operable solution, the condition $E-2U\cos\theta\le 0$ should hold.

Proof: The power flow equation of (C1) can be rearranged as

$$\begin{cases}EU\cos\left(\varphi+\theta\right)-U^2\cos\varphi=ZP_L \\ EU\sin\left(\varphi+\theta\right)-U^2\sin\varphi=ZQ_L\end{cases} \tag{C5}$$

where $\varphi=\tan^{-1}(x/r)$ and $Z=(r^2+x^2)^{1/2}$. Eliminating φ gives

$$\left(P_Lz+U^2\cos\varphi\right)^2+\left(Q_Lz+U^2\sin\varphi\right)^2=E^2U^2/z^2 \tag{C6}$$

Then, the voltage magnitude U can be obtained by solving

$$U^4+\left(2P_Lz\cos\varphi+2Q_Lz\sin\varphi-E^2\right)U^2+z^2\left(P_L^2+Q_L^2\right)=0 \tag{C7}$$

$$U=\sqrt{E^2/2-\left(P_Lz\cos\varphi+Q_Lz\sin\varphi\right)\pm\sqrt{\Delta}} \tag{C8}$$

with

$$\Delta=\left(2P_Lz\cos\varphi+2Q_Lz\sin\varphi-E^2\right)^2-4z^2\left(P_L^2+Q_L^2\right) \tag{C9}$$

It should be noted that if the power flow equation is stated in a high-voltage operable solution, the following condition should be valid:

$$U\ge\sqrt{E^2/2-\left(P_Lz\cos\varphi+Q_Lz\sin\varphi\right)} \tag{C10}$$

Substituting (C5) into (C10) yields

$$U^2\ge\left(E^2/2-\begin{pmatrix}\left(EU\cos\left(\varphi+\theta\right)-U^2\cos\varphi\right)\cos\varphi \\ +\left(EU\sin\left(\varphi+\theta\right)-U^2\sin\varphi\right)\sin\varphi\end{pmatrix}\right) \tag{C11}$$

$$U^2\ge E^2/2-EU\cos\theta+U^2\Rightarrow E-2U\cos\theta\le 0 \tag{C12}$$

(Q.E.D.)

Furthermore, according to (C4) and (C12), it can be concluded that, if the power flow is stated in a high-voltage solution (i.e., Eq. (C12) holds), the eigenvalues of (C4) can be derived as (i) $\lambda(J)\le 0$ if $x>0$; (ii) $\lambda(J)\ge 0$ if $x<0$.

Generally, it is widely considered in power systems that the reactance of each transmission line is positive (i.e., $x>0$), so the two eigenvalues of the Jacobian matrix of the *Single-Load*

Stiff-Bus system have negative real parts at the high-voltage solution. However, if there exists negative reactance (i.e., $x<0$), the real parts of the two eigenvalues will still be positive under the high-voltage condition. This has revealed that the traditional viewpoint on the negative real-part eigenvalues of the Jacobian matrix at a high-voltage operable solution does not necessarily hold due to the existence of the negative reactance.

REFERENCES

[1] K. Iba, H. Suzuki, M. Egawa, and T. Watanabe, "A method for finding a pair of multiple load flow solutions in bulk power systems," *IEEE Trans. Power Syst.,* vol. 5, no. 2, pp. 582-591, 1990.

[2] S. Zhao, H. Liu, S. Cheng, and D. Chen, "A new method for calculating power system multiple load flow solutions," in *Int. Conf. Advances in Power System Control, Operation and Management*, 1993, pp. 274-278.

[3] K. Okumura, T. Fujita, and A. Kijima, "Computation of multiple solution of load flow equation by simplicial subdivision homotopy method," *Electrical Engineering in Japan,* vol. 109, no. 1, pp. 31-39, 1989.

[4] P. Acharjee, and S. K. Goswami, "An Adaptive Particle Swarm Optimization Based Method for Normal and Low Voltage Multiple Load Flow Solutions," in *Joint Int. Conf. Power System Technology and IEEE Power India Conf.*, New Delhi, India, 2008, pp. 1-6.

[5] T. O. Ting, K. P. Wong, C.Y. Chung, "Locating Type-1 Load Flow Solutions using Hybrid Evolutionary Algorithm," *International Conference on Machine Learning and Cybernetics*, pp. 4093 - 4098, 2006.

[6] H. D. Nguyen, K. S. Turitsyn, "Appearance of multiple stable load flow solutions under power flow reversal conditions," *IEEE PES General Meeting*, National Harbor, MD, 2014.

[7] W. Xu, Y. Wang, "The Existence of Multiple Power Flow Solutions in Unbalanced Three-Phase Circuits," *IEEE Trans. Power Syst.*, vol. 18, no. 2, pp. 605-610, 2003.

[8] Y. Tamura, H. Mori, and S. Iwamoto, "Relationship Between Voltage Instability and Multiple Load Flow Solutions in Electric Power Systems," *IEEE Trans. Power App. Syst.,* vol. PAS-102, no. 5, pp. 1115-1125, 1983.

[9] K. Kawahara, N. Yorino, H. Sasaki, J. Kubokawa *et al.*, "An expert system for tracking multiple load flow solutions associated with voltage instabilities," in *Int. Conf. Advances in Power System Control, Operation and Management*, 1991, pp. 76-80 vol.1.

[10] H. D. Chiang, I. Dobson, R. J. Thomas, J. S. Thorp *et al.*, "On voltage collapse in electric power systems," *IEEE Trans. Power Syst.,* vol. 5, no. 2, pp. 601-611, 1990.

[11] P. W. Sauer, and M. A. Pai, "Power system steady-state stability and the load-flow Jacobian," *IEEE Trans. Power Syst.,* vol. 5, no. 4, pp. 1374-1383, 1990.

[12] C.-W. Liu, and J. S. Thorp, "A novel method to compute the closest unstable equilibrium point for transient stability region estimate in power systems," *IEEE Trans. Circuits Syst. I: Fundam. Theory and Appl.,* vol. 44, no. 7, pp. 630-635, 1997.

[13] N. Yorino, S. Harada, and H. Cheng, "A method to approximate a closest loadability limit using multiple load flow solutions," *IEEE Trans. Power Syst.,* vol. 12, no. 1, pp. 424-429, 1997.

[14] T. J. Overbye, and C. L. DeMarco, "Improved techniques for power system voltage stability assessment using energy methods," *IEEE Trans. Power Syst.,* vol. 6, no. 4, pp. 1446-1452, 1991.

[15] T. J. Overbye, and R. P. Klump, "Effective calculation of power system low-voltage solutions," *IEEE Trans. Power Syst.,* vol. 11, no. 1, pp. 75-82, 1996.

[16] T. O. Ting, K. P. Wong, and C. Y. Chung, "Locating Type-1 Load Flow Solutions using Hybrid Evolutionary Algorithm," in *Int. Conf. Machine Learning and Cybernetics*, Dalian, China, 2006, pp. 4093-4098.

[17] A. Shahriari, H. Mokhlis, A. H. A. Bakar, M. Karimi *et al.*, "The calculation of low voltage solution based on state space search method in ill-conditioned system," in *IEEE Int. Power Engineering and Optimization Conf.*, Melaka, Malaysia, 2012, pp. 62-66.

[18] C.-W. Liu, C.-S. Chang, J.-A. Jiang, and G. H. Yeh, "Toward a CPFLOW-based algorithm to compute all the type-1 load-flow solutions in electric power systems," *IEEE Trans. Circuits Syst. I,* vol. 52, no. 3, pp. 625-630, 2005.

[19] D. K. Molzahn, B. C. Lesieutre and H. Chen "Counterexample to a Continuation-Based Algorithm for Finding All Power Flow Solutions," *IEEE Trans. Power Syst.*, vol. 28, no. 1, pp. 564-565, 2013.

[20] R. D. Zimmerman, C. E. Murillo-Sánchez, and R. J. Thomas, "MATPOWER: Steady-State Operations, Planning, and Analysis Tools for Power Systems Research and Education," *IEEE Trans. Power Syst.,* vol. 26, no. 1, pp. 12-19, Feb. 2011.

[21] J. H. Harlow, *Electric power transformer engineering*: CRC press, 2007.

[22] A. A. Mazi, B. F. Wollenberg, and M. H. Hesse, "Corrective Control of Power System Flows by Line and Bus-Bar Switching," *IEEE Trans. Power Syst.,* vol. 1, no. 3, pp. 258-264, 1986.

[23] B. Stott, and O. Alsac, "Fast Decoupled Load Flow," *IEEE Trans. Power App. Syst.,* vol. PAS-93, no. 3, pp. 859-869, 1974.

[24] P. S. N. Rao, K. S. P. Rao, and J. Nanda, "An Empirical Criterion for the Convergence of the Fast Decoupled Load Flow Method," *IEEE Trans. Power App. Syst.,* vol. PAS-103, no. 5, pp. 974-981, 1984.

[25] R. Bhatia, *Positive definite matrices*. Princeton Series in Applied Mathematics, 2007.

[26] R. A. Horn, *Matrix Analysis*. Cambridge University Press, 1990.

[27] H.-D. Chiang, A. J. Flueck, K. S. Shah, and N. Balu, "CPFLOW: a practical tool for tracing power system steady-state stationary behavior due to load and generation variations," *IEEE Trans. Power Syst.,* vol. 10, no. 2, pp. 623-634, 1995.